

# HYDROGEN SORPTION AND ELECTROCHEMICAL PROPERTIES OF INTERMETALLIC COMPOUNDS $\text{La}_2\text{Ni}_7$ AND $\text{La}_2\text{Ni}_6\text{Co}$

E. LEVIN, P. DONSKOY, S. LUSHNIKOV, V. VERBETSKY,  
T. SAFONOVA, O. PETRII  
*Moscow State University*  
*Chemistry Department*  
*Leninskie Gory 3, Moscow, 119992 Russia*  
*E-mail: levin@elch.chem.msu.ru*

## Abstract

Intermetallic compounds (IMCs)  $\text{La}_2\text{Ni}_7$  and  $\text{La}_2\text{Ni}_6\text{Co}$  were obtained by arc melting technique followed by annealing. Samples were characterized by means of X-ray powder diffraction (XRD). Crystal structure of  $\alpha\text{-La}_2\text{Ni}_7$  was refined using single crystal X-ray data. Hydrogen desorption isotherms were obtained for  $\text{La}_2\text{Ni}_7$  and  $\text{La}_2\text{Ni}_6\text{Co}$  at  $T=273\text{K}$  and  $T=295\text{K}$ . Electrochemical discharge properties of  $\text{La}_2\text{Ni}_7$  and  $\text{La}_2\text{Ni}_6\text{Co}$  were investigated. The introduction of Co in alloy led to decreasing of hydride equilibrium pressure.

**Keywords:** nickel-metal hydride battery, hydrogen storage alloy, discharge capacity, single crystal X-ray diffraction, crystal structure

## 1. Introduction

At present, in line with the increasing demand for portable batteries, active studies are carried out in a search for new compounds for optimization of electrode materials. One type of such batteries is nickel metal hydride (MH) batteries. These batteries are widely applied today because of their high energy density, recycling possibility and environmental safety. This paper deals with materials for negative electrodes for Ni-MH batteries. For this purposes wide range of compounds are in use [1-4]. For our studies we have chosen two  $\text{Ce}_2\text{Ni}_7$ -type [5] compounds:  $\text{La}_2\text{Ni}_7$  and  $\text{La}_2\text{Ni}_6\text{Co}$  which had never been tested for their electrochemical properties. Crystal structure of  $\text{La}_2\text{Ni}_7$  was refined using single crystal X-ray data. Hydrogen sorption and electrochemical properties were investigated.

## 2. Experimental

Alloys were prepared using arc-melting technique from the mixtures of initial metals under argon atmosphere. As known [6], La-based compounds of this structure type are bimorphic, hence all compounds were annealed for 240 h at 1153K to reach homogeneity and for low temperature phase stabilisation. The phase composition of alloys was determined using X-ray powder diffraction data. X-Ray powder diffraction (XRD) patterns were taken at room temperature by using a DRON 3M diffractometer

( $\text{CuK}_\alpha$  radiation, graphite monochromator) in the range of  $2\theta=20^\circ\text{-}80^\circ$  with a step of  $0.05^\circ$ . Single crystal diffraction data were collected at room temperature on Enraf-Nonius CAD-4 diffractometer. Structure was refined with JANA-2000 program package [7]. The results of data collection and structure refinement are summarized in Table 1.

Pressure-composition isotherms were obtained using Siewert's type apparatus at a pressure below 25 atm. The samples were hydrogenated by step-by-step pressure increasing. Absorption isotherms were not recorded.

The electrodes for electrochemical experiments were prepared by mixing alloy powder with copper powder in weight ratio 1:4. The mixture was cold-pressed to a 7-mm pellet at a pressure  $150\text{ atm/cm}^2$ . All electrochemical experiments were carried out using a three-electrode quartz cell with Hg/HgO as the reference electrode, Pt wire as the counter electrode, and MH as the working electrode. The electrolyte was 6M KOH. For measurements, a P-5827M potentiostat was used. The data were collected using X-Y recorder. The cut-off potential was  $-0.6\text{V}$ .

TABLE 1. Summary of crystallographic information for  $\text{La}_2\text{Ni}_7$

Estimated chemical formula	$\text{La}_2\text{Ni}_7$
Crystal system	Hexagonal
Space group	$\text{P6}_3/\text{mmc}$
Cell constants $a, c$ ( $\text{\AA}$ )	5.0577(4) 24.7336(22)
Volume ( $\text{\AA}^3$ )	547.926
$Z$	4
$D_{\text{calc}}$ , $\text{g}\cdot\text{cm}^{-3}$	8.345
Radiation/ Wavelength ( $\text{\AA}$ )	$\text{MoK}_\alpha/0.71073$
$\theta$ range ( $^\circ$ ) for cell determination	9.47 – 22.39
Linear absorption coefficient ( $\text{cm}^{-1}$ )	38.54
Temperature (K)	293
Crystal shape	Arbitrary
Colour	Metallic
Diffractometer	CAD4, Graphite monochromator
Data collection method	$\omega$ - $\theta$
Absorption correction	Rocking curve
No. of measured reflections	3653
No. of observed independent reflections	388
Criteria for observed reflections	$I > 3\sigma(I)$
Data collection $\theta$ limits ( $^\circ$ )	2 – 35

Range of $h, k, l$	$0 \rightarrow h \rightarrow 8, -8 \rightarrow k \rightarrow 8, -39 \rightarrow l \rightarrow 39$
$R_{int}$	0.025
Refinement on	F
Extinction	Anisotropic, Becker-Coppens, Type I, Gaussian distribution
$R/R_w$ ( $I > 3\sigma(I)$ )	0.042/0.063
Goodness of fit	1.01
No. of reflections used in refinement	386
No. of refined parameters	26
Weighting scheme	$w = (\sigma^2(F) + (0.045F)^2)^{-1}$
$(\Delta/\sigma)_{max}$	0.004
$\Delta \rho_{max}$ ( $e/\text{\AA}^{-3}$ ) +/-	+3.47/-4.18

### 3. Results and discussion

XRD patterns of alloy powders are given in Figure 1. Comparison of experimental and calculated patterns revealed absence of impurities in samples.

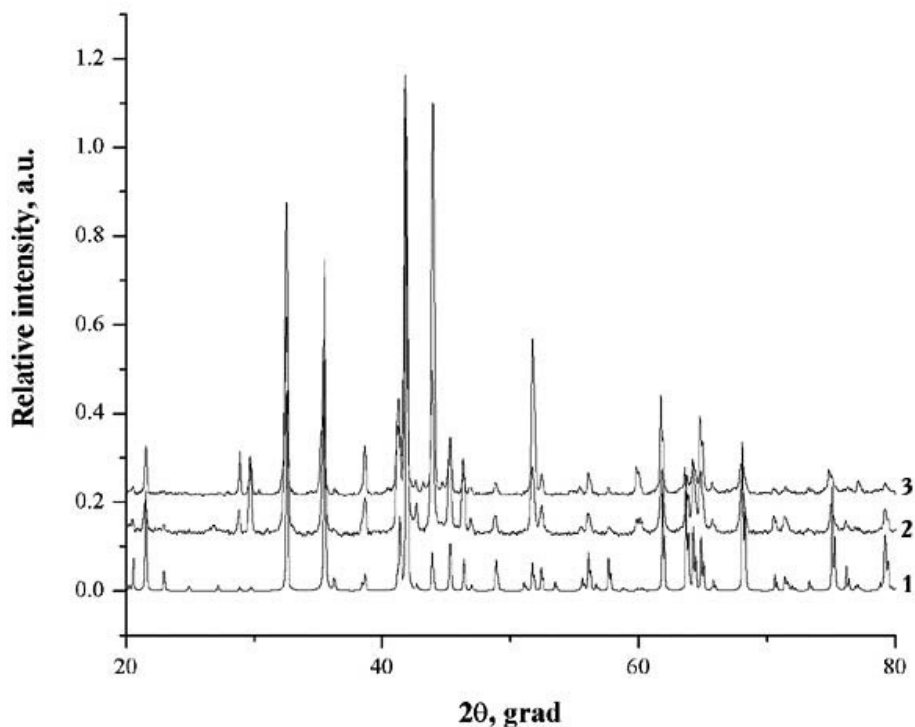


Figure 1. XRD patterns of obtained samples: 1 - calculated pattern for  $\text{La}_2\text{Ni}_7$ , 2 - experimental pattern for  $\text{La}_2\text{Ni}_7$ , 3 - experimental pattern for  $\text{La}_2\text{Ni}_6\text{Co}$ .

Structure refinement was carried out using the model from [5]. Coordinates and atomic displacement parameters (ADP) are given in Table 2. Refinement with isotropic temperature factors converged at  $R=0.042$ ,  $wR=0.063$  and in case of anisotropic temperature factors refinement resulted in  $R=0.035$ ,  $wR=0.049$ . Unfortunately, rocking curve method does not produce perfect absorption correction; and, thus, the refinement produced slightly negative atomic displacement tensors for two Ni atoms, so they are not listed. During refinement we detected no significant differences from [5] in atomic site parameters and no structure peculiarities. All temperature factors were at least two times lower as compared with those given in [5]. Refined atomic coordinates and ADPs are summarised in Table 3.

TABLE 2. Atomic coordinates and ADPs from Cromer, D. [5].

Atomic Site	Site symmetry	x	Y	z	$B_{iso}, \text{\AA}^2 *$
Ce1	4f	1/3	2/3	0.0302(2)	0.62(7)
Ce2	4f	1/3	2/3	0.1747(2)	0.61(6)
Ni1	2a	0	0	0	0.50(21)
Ni2	4e	0	0	0.1670(4)	0.64(16)
Ni3	4f	1/3	2/3	0.8334(4)	0.60(14)
Ni4	6h	0.8351(18)	0.6702(18)	1/4	0.41(8)
Ni5	12k	0.8338(14)	0.6676(14)	0.0854(2)	0.67(7)

TABLE 3. Refined atomic coordinates and ADPs.

Atomic site	Site symmetry	x	y	z	$B_{iso}, \text{\AA}^2$
La1	4f	1/3	2/3	0.03013(3)	0.19(2)
La2	4f	1/3	2/3	0.17422(3)	0.20(2)
Ni1	2a	0	0	0	0.22(4)
Ni2	4e	0	0	0.16898(7)	0.30(3)
Ni3	4f	1/3	2/3	0.83616(8)	0.29(3)
Ni4	6h	0.8341(3)	0.6682(1)	1/4	0.11(2)
Ni5	12k	0.8350(2)	0.6700(1)	0.08806(4)	0.16(2)

Pressure-composition-temperature curves were measured for  $T=273\text{K}$  and  $T=295\text{K}$ . From these data, pressure-composition isotherms were plotted. Figures 2, 3 show the isotherms for  $\text{La}_2\text{Ni}_7$  and for  $\text{La}_2\text{Ni}_6\text{Co}$  at equal temperatures. Starting point of desorption isotherms was determined from values of hydrogen sorbed. As seen from these figures, equilibrium hydride pressure decreases with an introduction of Co into

alloy, but even for  $\text{La}_2\text{Ni}_6\text{Co}$  the equilibrium pressure is higher than 1 atm. From these isotherms we can see, that at  $T=273\text{K}$  the plateaus have an increased slope as compared with isotherms taken at room temperature (295 K). Also hydrogen does not desorb totally. These facts can be explained by the slow kinetics of reaction of IMCs with hydrogen at lowered temperatures, which is revealed in the increasing slope that indicating a nonequilibrium process. For clarifying these phenomenon the hydrogen desorption rate should be slower. But for primary estimation of hydrogen-sorption properties we can use already obtained data.

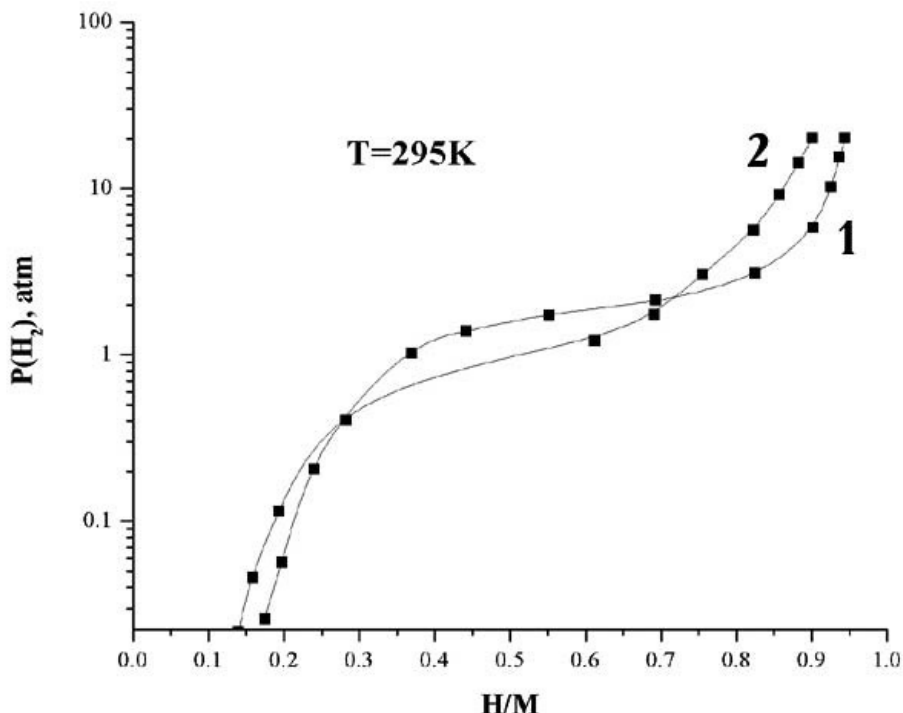


Figure 2. Hydrogen desorption isotherms at  $T=295\text{ K}$ . 1 –  $\text{La}_2\text{Ni}_7$ , 2 –  $\text{La}_2\text{Ni}_6\text{Co}$ .

As far as we know, there is only one article dealing with La-based hydrides of such a structure type [8]. Although the values of hydrogen absorbed well agree with these in literature ( $H/M=0.89$  from [8] and  $H/M=0.94$  from our absorption data) there is no previously reported data concerning pressure values of absorption or desorption at all.  $H/M=0.94$  value obtained for  $\text{La}_2\text{Ni}_7$  is close to that well known for  $\text{LaNi}_5$   $H/M=1$ . Although our compound contains more rare-earth metal than  $\text{LaNi}_5$ -type alloys it would be very interesting to investigate Ce-based compounds of such type. There is also only one article dealing with  $\text{Ce}_2\text{Ni}_7$  and its Co derivative [9]. These data indicate that the equilibrium pressure of Ce-based compounds is very low ( $\sim 0.01$  atm). On the other hand, introducing Ce into  $\text{AB}_5$ -type alloys leads to catastrophic increasing [10] of equilibrium pressure. Inasmuch as all commercial rare-earth containing alloys are based on mischmetal, compounds of the  $\text{Ce}_2\text{Ni}_7$ -type can be a cheaper alternative to  $\text{LaNi}_5$ -based compounds. But this question needs more attention and further investigation.

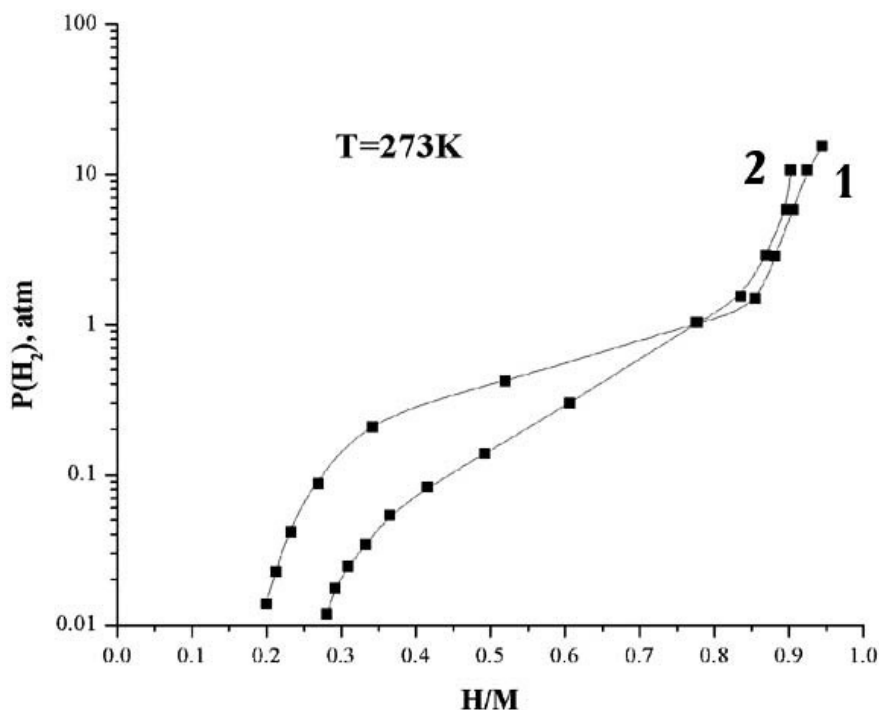


Figure 3. Hydrogen desorption isotherms at  $T=273$  K. 1 –  $\text{La}_2\text{Ni}_7$ , 2 –  $\text{La}_2\text{Ni}_6\text{Co}$ .

Figure 4 shows the electrochemical discharge curves at current density  $j=100$  mA/g and corresponding sections of desorption isotherms at  $T=295$  K. Pressure for discharge curves was calculated using the Nernst equation. As we can see, electrochemical curves are much shorter in terms of H/M ratio than desorption isotherms. This is caused by high dissociation pressure for  $\text{La}_2\text{Ni}_7$  and  $\text{La}_2\text{Ni}_6\text{Co}$  which results in incomplete adsorption-desorption in electrochemical conditions. Moreover, in the discharge curve for  $\text{La}_2\text{Ni}_7$ , two regions with different slopes exist. The upper (in term of equilibrium pressure) plateau corresponds to  $\alpha \leftrightarrow \beta$  hydride phase transition. The presence of the second plateau can be explained by the contribution of hydrogen ionization. We can suggest that no quantitative measurements can be made on such samples without altering chemical composition in order to low equilibrium pressure.

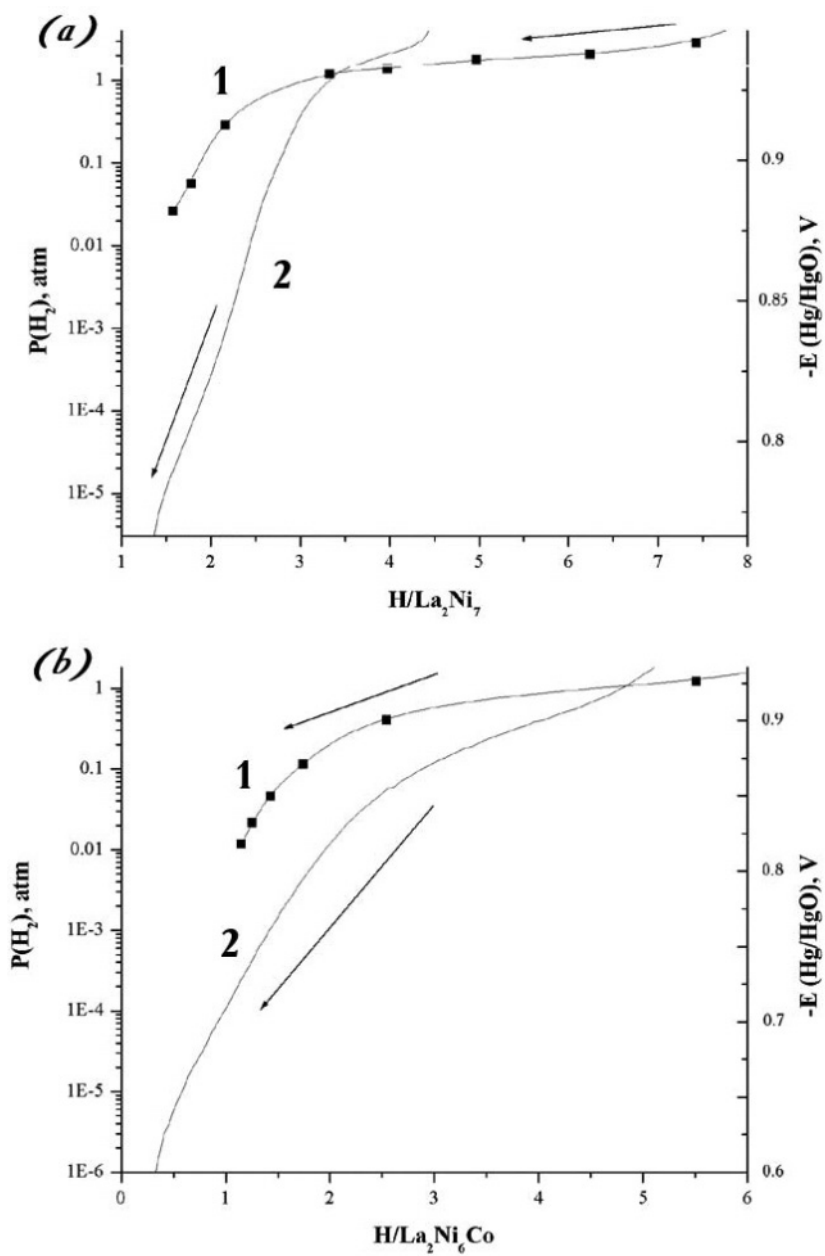


Figure 4. Electrochemical discharge curves and corresponding sections of desorption isotherms; a ( $\text{La}_2\text{Ni}_7$ ): 1 – desorption isotherm, 2 – discharge curve; b ( $\text{La}_2\text{Ni}_6\text{Co}$ ): 1 – desorption isotherm, 2 – discharge curve.

#### 4. Conclusions

Thus, the studied  $\text{Ce}_2\text{Ni}_7$ -type alloys showed relatively high hydrogen adsorption capacities, but low electrochemical discharge capacities. This correlates with high equilibrium pressure of the La-based hydrides. Introduction of Co into the alloy led to decreasing of the equilibrium pressure. Probably, the introduction of pressure-reducing elements, such as Ce, Mn, V can be promising.

#### 5. Acknowledgements

We are grateful to Mironov A.V. for his help in carrying out single crystal experiments and for censorious remarks during discussion.

#### 6. References

1. Petrii, O., Vasina, S., Korobov, I. (1996) Electrochemistry of hydride-forming intermetallic compounds and alloys, *Usp. Khim.* **65**(3), 195-210 (in Russian).
2. Kleperis, J., Wojcik, G., Czerwinski, A., Skowronski, J., Kopczyk, M., Beltowska-Brzezinska, M. (2001) Electrochemical behavior of metal hydrides, *Solid State Electrochem.* **5**, 229-249.
3. Sakai, T., Matsuoka, M., Iwakura, C. (1995) Handbook of the Physics and Chemistry of Rare Earths, Elsevier, Amsterdam, 138-180.
4. Fuller, T., Newman, J. (1995) Modern Aspects of Electrochemistry, Plenum Press, New York, 359-382.
5. Cromer, D., Larson, A. (1959) The crystal structure of  $\text{Ce}_2\text{Ni}_7$ , *Acta Cryst.* **12**, 855-858.
6. Okamoto, H. (2002) La-Ni (Lanthanum-Nickel), *J. Phase Equilibria*, **23**(3), 287-288.
7. Petricek, V., Dusek, M. (2000). *Jana2000. The crystallographic computing system.* Institute of Physics, Praha, Czech Republic.
8. Maeland, A., Andressen A., Videm, K. (1976) Hydrides of lanthanum-nickel compounds, *J. Less-Common Met.*, **45**, 347-350.
9. Van Essen, R., Buscow, K. (1980) Hydrogen sorption of Ce-3d and Y-3d intermetallic compounds, *J. Less-Common Met.*, **70**, 189-198.
10. Klyamkin, S., Verbetsky, V., Karih, A. (1995) Thermodynamic particularities of some  $\text{CeNi}_5$ -based metal hydride systems with high dissociation pressure, *J. Alloys Comp.*, **231**, 479-482.